Available online at www.sciencedirect.com

ScienceDirect

Optical Materials 30 (2008) 1560–1566

OPTICAL Materials

www.elsevier.com/locate/optmat

# Exploration of waveguide fabrication from thermally evaporated Ge–Sb–S glass films

Juejun Hu [a], Vladimir Tarasov [a], Nathan Carlie [b], Laeticia Petit [b], Anu Agarwal [a,*], Kathleen Richardson [b], Lionel Kimerling [a]

[a] *Microphotonics Center, Massachusetts Institute of Technology, Rm 13-4126, 77 Mass Avenue, Cambridge, MA 02139, USA*

[b] *Advanced Materials Research Laboratory, Clemson University, USA*

Received 20 July 2007; received in revised form 25 September 2007; accepted 8 October 2007
Available online 28 November 2007

**Abstract**

Waveguides from thermally evaporated $Ge_{23}Sb_7S_{70}$ films have been fabricated using both plasma etching and lift-off techniques. The two methods have been compared in their ability to provide high quality, low-loss waveguides for microphotonics applications. We have demonstrated in this paper that low-loss 3 μm and 4 μm wide channel waveguides can be fabricated using $CHF_3$ and $SF_6$ plasma etching, and lift-off, respectively. Additionally, lift-off does not change the structure of the waveguide during the fabrication whereas the structure of the plasma etched waveguide differs slightly from that of the films. Finally, channel waveguides fabricated using lift-off leads to a low RMS roughness of $10 \pm 2$ nm, compared to those fabricated by a plasma etching process which lead to a higher RMS roughness of 17–20 nm. As-fabricated waveguides have been found to exhibit optical propagation losses of 3–5 dB/cm at 1550 nm. These high losses are attributed to scattering by sidewall roughness and defects arising from the fabrication process.
© 2007 Elsevier B.V. All rights reserved.

*PACS:* 42.82.E; 52.75.R; 42.70.C; 78.66.J

*Keywords:* Chalcogenide films; Waveguide fabrication; Raman spectroscopy; Plasma etching; Lift-off; Waveguide loss

## 1. Introduction

Amorphous chalcogenide glasses (ChG's) are of great interest to researchers because of their flexible structure, wide range of properties, capacity for doping, and especially their ability to transmit light in the mid to far-infrared region of the spectrum [1]. The infrared transparency of chalcogenide glasses allows their use in optical fibers for transmission of light generated by CO and $CO_2$ lasers operating in the infrared [2], and such fibers are applied towards high-precision tools in surgery and industrial cutting and welding [1]. As their planar counterparts, chalcogenide waveguides have seen use in evanescent sensing [3], because they are capable of delivering an infrared spectrum from a Fourier Transform Infrared (FTIR) spectrometer to an atmosphere of interest and returning the absorption spectrum to a detector, essentially acting as a remote FTIR spectrometer. Additionally, these waveguides have been fabricated in several glass compositions using techniques including direct laser writing [4], wet etching [5], plasma etching [6] and lift-off [7], and have found wide applications in fields such as light emission [8], nonlinear optics [9], all-optical switching [10] and chemical sensing [11].

Plasma etching and lift-off techniques have both been successfully utilized to patterns device in many material systems such as Si, $SiO_2$ and $Si_3N_4$; the two methods have their distinct features and advantages. By selecting an appropriate plasma etching chemistry and fine-tuning the recipe, it is possible to yield different sidewall profiles according to specific device requirements [12]. However, chalcogenide films can be attacked by commercial

* Corresponding author. Tel.: +1 617 253 5302; fax: +1 617 253 6782.
*E-mail address:* anu@mit.edu (A. Agarwal).

0925-3467/$ - see front matter © 2007 Elsevier B.V. All rights reserved.
doi:10.1016/j.optmat.2007.10.002

($NH_4OH$)-based developers, which may lead to severe film peeling [5], and thus in this paper we developed specialty photolithography and etching protocols to resolve this issue; whereas in the case of lift-off, direct contact between developer and glass film is avoided. Each method is distinct in its feature generation and mechanical and chemical treatment of the patterns. The plasma etching protocol calls for more stringent restrictions in thermal and chemical treatment of these glasses, whose high atomic masses and weak interatomic bonds lead to highly process-sensitive properties. Furthermore, due to the fact that chalcogenide materials are not currently regarded as CMOS-compatible, plasma etching techniques require dedicated lithography and etching facilities to avoid contamination in a CMOS foundry. In contrast, the lift-off technique minimizes the need for dedicated machines and significantly reduce fabrication cost and is applicable to patterning of different chalcogenide compositions, even the ones that are not amenable to the plasma etching technique. These reasons make lift-off technique a highly versatile technique for both rapid prototyping and mass production in the fabrication of planar chalcogenide devices.

The $Ge_{23}Sb_7S_{70}$ glass network has been chosen as the waveguide material in this study as this system has a wide infrared transparency window as well as low toxicity compared to arsenic based chalcogenide glass system, is well-characterized [13–15], and is relatively easy to prepare in bulk and film forms. Films have been deposited from this bulk glass using thermal evaporation and pulsed laser deposition techniques. The results from a detailed study of the optical and structural properties of $Ge_{23}Sb_7S_{70}$ are published separately [16].

In this paper, we present the fabrication and characterization of chalcogenide glass $Ge_{23}Sb_7S_{70}$ channel waveguides using both plasma etching and lift-off techniques. The films used in this study have been deposited on an oxide-coated Si wafer substrate by a thermal evaporation technique from a chalcogenide glass, $Ge_{23}Sb_7S_{70}$, used as an evaporant. Chalcogenide composition and structural characteristics before and after waveguide fabrication have been compared using wavelength dispersive spectroscopy (WDS), Raman spectroscopy and X-ray diffraction (XRD) techniques. Waveguide loss has been measured using fiber coupling and sidewall roughness has been evaluated using atomic force microscopy (AFM). Simulation of the optical mode profile has been performed and compared to the measurement.

## 2. Device fabrication

### 2.1. Film deposition

Bulk $Ge_{23}Sb_7S_{70}$ glass for film deposition is prepared from high purity elements using a traditional melt-quenching technique. Details of the bulk sample preparation process may be found elsewhere [14]. $Ge_{23}Sb_7S_{70}$ glass films are then thermally deposited onto substrates in an Edwards E306A single-source evaporator. The substrates are 6 in. Si wafers pre-coated with a 3 μm-thick thermal oxide (Silicon Quest International Inc.). For waveguides fabricated by plasma etching, chalcogenide films are deposited directly onto the substrates. These films are subsequently patterned using standard photoresist before plasma etching. For the lift-off process, reverse photoresist patterns are formed on the substrates prior to chalcogenide deposition. The film is deposited at a base pressure of $4 \times 10^{-7}$ Torr using a tantalum baffled source and the deposition rate is estimated to be $\sim 50$ /s.

### 2.2. Waveguide fabrication by plasma etching

$Ge_{23}Sb_7S_{70}$ coated wafers are spin-coated with commercial photoresist (OCG-825) on a Headway spinner at 2000 rpm. No photoresist adhesion promoter is used during the processing, since the adhesion of the baked resist to the glass is sufficient to survive development and subsequent glass etching without peeling. A 10 min bake at 130 °C follows. The purpose of the relatively high temperature bake (with respect to the regular soft bake temperature of 90 °C) is to decrease the photosensitivity of the photoresist and thus allows accurate control of the resist dissolution rate during development. Optical microscope inspection of the resist layer reveals no cracking after the baking. Subsequent UV exposure is carried out on a Karl Suss MJB3 aligner. A commercially available developer (OCG 934 1:1) is used to develop the resist. In order to prevent wet etching by the developer and the resulting undercut and film peeling, the development is stopped before the resist layer is fully developed by controlling the development time. The remaining thin layer of undeveloped photoresist is then etched by oxygen plasma in a dual chamber PlasmaTherm plasma etcher, followed by a reactive fluorine ion etch in the same chamber to define the waveguide patterns.

To fabricate the waveguide using plasma etching, four different gas chemistries, $O_2$, Ar, $CHF_3$ and $SF_6$, are tested. Etch rates of the recipes are monitored off-line using a Dektak IIA surface profiler and are tabulated in Table 1. The gas flow rate, pressure and incident RF power are optimized to yield vertical sidewall profiles and good pattern fidelity. Both fluorine chemistries are effective in glass etching, while $Ge_{23}Sb_7S_{70}$ is almost inert in an oxygen plasma.

After extended exposure (e.g. $\sim$15 min) to reactive plasma (except for $O_2$, which ashes the photoresist), the photoresist denatures and becomes virtually impossible to remove after etching, either by oxygen plasma or by sonication in organic solvents such as acetone, which was confirmed by other similar studies [17]. Thus even though Ar ion milling has previously been used to pattern ridge waveguides in $GeS_2$ film [18], our study reveals that it is an inefficient method for etching $Ge_{23}Sb_7S_{70}$ films, which only allows fabrication of shallow ridge waveguides due to its slow etch rate. Based on this consideration, the $CHF_3$ and $SF_6$ recipes in Table 1 are employed for actual waveguide fabrication in this study. Channel waveguides with

Table 1
Plasma etching conditions and etch rates of $Ge_{23}Sb_7S_{70}$ film in $CHF_3$, $SF_6$, Ar and $O_2$ gas chemistries

| Gas chemistry | Flow rate (sccm) | Pressure (mTorr) | Incident power (W) | Etch rate (nm/min) |
|---|---|---|---|---|
| $CHF_3$ | 40 | 30 | 350 | $60 \pm 10$ |
| $SF_6$ | 40 | 30 | 350 | $300 \pm 30$ |
| $O_2$ | 40 | 30 | 350 | $\sim 3$ |
| Ar | 40 | 40 | 250 | $23 \pm 3$ |

two different core widths, 3 μm and 4 μm, are patterned using both plasma etching recipes. Residual photoresist is removed by an oxygen plasma. A 20 μm thick layer of SU8 (SU8 2015, Microchem Inc.) is then spin-coated onto the wafer to serve as the waveguide upper cladding. A schematic of the process flow is shown in Fig. 1a.

### 2.3. Waveguide fabrication by lift-off

In the lift-off process, instead of etching chalcogenide films directly, a photoresist pattern is formed on blank oxide-coated Si wafers via a traditional photographic process similar to that in plasma etching. $Ge_{23}Sb_7S_{70}$ is then thermally evaporated onto the wafer patterned with photoresist, and sonicated in solvent (usually acetone) to dissolve the photoresist beneath the $Ge_{23}Sb_7S_{70}$ film and to "lift-off" the chalcogenide layer. Only $Ge_{23}Sb_7S_{70}$ deposited onto areas not covered by photoresist is retained, and thus a chalcogenide pattern reverse that of the photoresist is defined. The patterned wafer is then rinsed in methanol and isopropanol to clean the surface. Commercially available negative photoresist NR7-1000P is used for $Ge_{23}Sb_7S_{70}$ lift-off due to its negative-sloping sidewall profile, which facilitates the lift-off process. The channel waveguides are then clad by a 20 μm thick layer of spin-coated SU8 polymer. A schematic of the process flow is shown in Fig. 1b.

## 3. Experimental characterization

### 3.1. Material structure characterization

Raman spectroscopy is used as a powerful tool to probe the glass network structures. The Raman spectra are recorded with a Kaiser Hololab 5000R Raman spectrometer with Raman microprobe attachment in backscattering geometry. This system has a typical resolution of 2–3 $cm^{-1}$ at room temperature. The system consists of a holographic notch filter for Rayleigh rejection, a microscope equipped with 10×, 50× and 100× objectives (the latter allowing Raman spectra to be collected from spot sized down to 5–7 μm), and a CCD detector. A 785 nm NIR semiconductor diode laser is used for excitation. The use of a 785 nm source with a low excitation power of ~5 mW is specific to our study to avoid photo-structural changes which the laser beam may induce in the samples during measurement. The spectral measurements are repeated on several different locations on the films and the resultant spectra are numerically averaged to eliminate any impact from film non-uniformity.

### 3.2. Device characterization

The morphology of as-fabricated $Ge_{23}Sb_7S_{70}$ waveguides is characterized using a JEOL 6320FV field-emission high-resolution SEM.

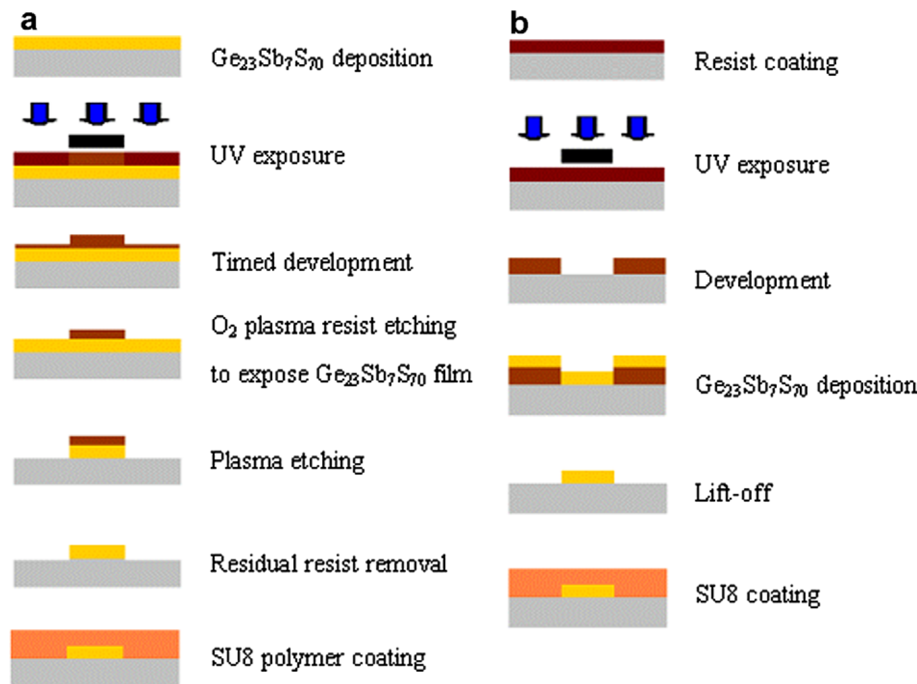


Fig. 1. Process flow schematics of waveguide fabrication using (a) $CHF_3$ plasma etching, (b) $SF_6$ plasma etching and (c) the lift-off process.

A digital instruments nanoscope IIIa atomic force microscope (AFM) is used to measure the roughness of the $Ge_{23}Sb_7S_{70}$ waveguides. Measurement scans are performed parallel to the direction of the waveguides using the tapping mode.

Waveguide mode profiling and loss measurements are performed on a Newport AutoAlign workstation. Lens-tip fibers are used to couple laser light into and out of the waveguides. Highly reproducible coupling between waveguides and fibers is achieved via an automatic alignment system.

Optical modes from the waveguides are profiled by measuring the output optical power as a function of output coupling fiber tip position.

Waveguide loss is determined via a standard cutback method using paper-clip waveguide patterns on the same Newport AutoAlign measurement system.

## 4. Results and discussion

In this paper, chalcogenide waveguides are fabricated using plasma etching and lift-off techniques. Compositional analysis and the optical and structural characterization of the chalcogenide waveguides are performed, and compared, to identify the optimal technique for low loss chalcogenide waveguide fabrication.

### 4.1. Compositional analysis and structural characterization

The optical and structural properties of the film deposited by thermal evaporation have been investigated and are published separately [16]. The as-evaporated film composition is slightly non-stoichiometric compared to the bulk source. Micro-Raman spectroscopy reveals that the structure of the film is similar to that of the bulk glass, but not identical. The glass network of the film is expected to have a higher number of edge and corner-sharing $GeS_4$ units compared to the network of the corresponding bulk.

Waveguides are fabricated using plasma etching and lift-off techniques as described previously. The amorphous nature, of the as-deposited and patterned films, is confirmed by X-ray diffraction. Neither crystallization peaks nor diffraction spectra changes are observed for patterned films, indicating the absence of major crystallization and structural modification induced by processing. Wavelength dispersive spectroscopy (WDS) composition analysis carried out on a JEOL JXA-733 superprobe reveals that the resulting waveguides have the same composition as the as-deposited film within the accuracy of the measurement.

The measured Raman spectra of the as-deposited and patterned $Ge_{23}Sb_7S_{70}$ films, shown in Fig. 2, are in good agreement with previous studies of the Ge–Sb–S glass system [14]. The Raman spectra present a broad band with 2 bands of low amplitude in the 200–250 $cm^{-1}$. In accordance with Mei et al, the bands at 330 and 402 $cm^{-1}$ have been assigned to the $A_1$ and $T_2$ modes of corner sharing $GeS_{4/2}$ groups [19]. The bands at 340, 375 and 427 $cm^{-1}$ have been attributed, respectively to $A_1$ mode of the $GeS_4$ molecular units [20], to the $T_2$ mode of 2 edge-sharing $GeS_{4/2}$ tetrahedra and to the vibration of two tetrahedra connected through a bridging sulfur $S_3Ge–S–GeS_3$. The shoulder at around 302 $cm^{-1}$ has been assigned to the E modes of $SbS_3$ pyramids [21], which, however, in this case becomes indistinguishable with the contribution from the Si wafer substrate band at $\sim$305 $cm^{-1}$. The bands in the range 175–225 $cm^{-1}$ have been attributed to $A'_1$ mode of a six-membered ring and also to the vibration of Ge–S–Ge dithiogermanate. The shoulder at 250 $cm^{-1}$ in the films can be attributed the vibrations of "wrong-bonds" in the glass network, such the Ge–Ge bond in the ethane-like unit $S_3Ge–GeS_3$ [22]. As one would expect, lift-off does not lead to observable structural modifications in the waveguide, since no thermal or chemical processing steps are involved in the patterning process. In contrast, one can notice slight variations of the Raman spectrum after both plasma etching processes. In order to understand the structure variation, the spectra are fitted keeping the position and the bandwidth of the peak constant. Fig. 2e shows an example of the deconvoluted Raman spectra, taken from as-deposited $Ge_{23}Sb_7S_{70}$ film and Table 2 summarizes the peak deconvolution results of the Raman spectra. One can notice that the ratio of the band at 295 $cm^{-1}$ decreases and the one at 340 $cm^{-1}$ increases when the waveguide is made by plasma etching suggesting a lower number of $SbS_3$ units and higher number of isolated $GeS_4$ units in the structure of the waveguide. Nevertheless, we believe that such structural variations are not a major concern for waveguide loss reduction, given the small degree of Raman spectra variation.

### 4.2. Waveguide characterization

The sidewall angles of the fabricated waveguides are observed using SEM and the pictures are exhibited in Fig. 3. The waveguides fabricated using plasma etching have similar sidewall angles. As seen in Fig. 3a, the waveguides patterned by fluorine ion etching showed vertical sidewall angle which can be attributed to the formation of polymer protective coatings on feature sidewalls during plasma etching [23]. In contrast, lift-off features lead to a sidewall angle of $\sim$70°, as demonstrated by rounded corners in Fig. 3b.

Surface profiles of as-fabricated waveguides are measured by AFM and analyzed using the Digital Instruments Nanoscope Software. The RMS sidewall roughness values for $Ge_{23}Sb_7S_{70}$ waveguides patterned by $CHF_3$ plasma etching, $SF_6$ plasma etching and lift-off are $20 \pm 5$ nm, $17 \pm 4$ nm and $10 \pm 2$ nm, respectively.

As an example, Fig. 4a and b show, respectively, the measured optical modal profile from a 3 μm wide channel waveguide patterned by $SF_6$ plasma etching, and the numerically simulated optical mode in the same waveguide obtained from a finite-difference technique [24]. Similarly

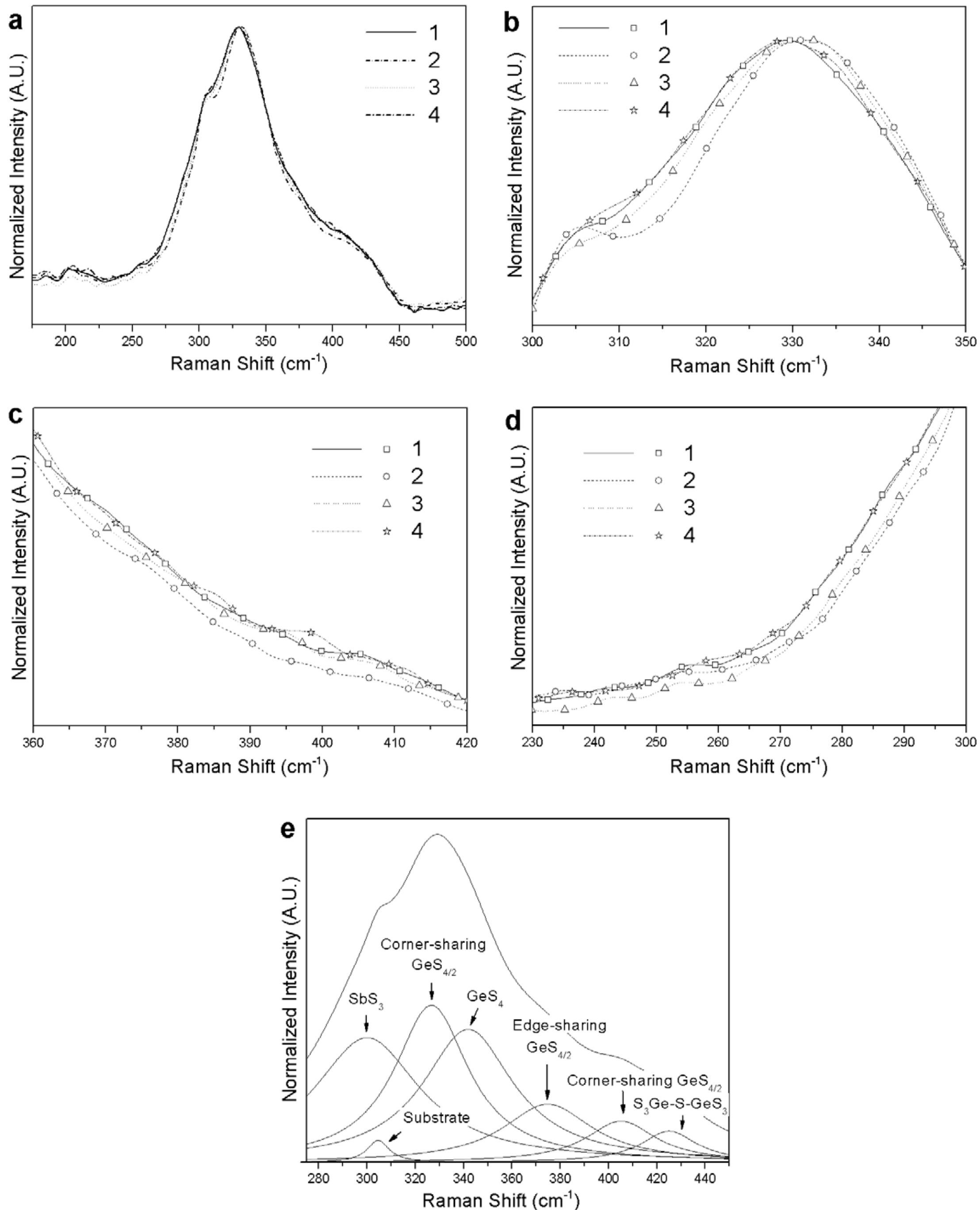


Fig. 2. (a)–(d) Raman spectra of (1) as-deposited $Ge_{23}Sb_7S_{70}$ film; (2) $Ge_{23}Sb_7S_{70}$ waveguide patterned by $CHF_3$ plasma etching; (3) $Ge_{23}Sb_7S_{70}$ waveguide defined by $SF_6$ plasma etching; (4) $Ge_{23}Sb_7S_{70}$ waveguide fabricated by lift-off; (e) as-deposited $Ge_{23}Sb_7S_{70}$ film with peak deconvolution result.

good agreement between simulation and experiment is observed for a 3 μm wide waveguide. The measured mode size (defined as the area where the optical field intensity is greater than $1/e$ of the peak intensity, where $e = 2.718$) is 2.5 μm × 1.1 μm, in contrast to the simulation result of 2.7 μm × 0.9 μm. The slight deviation can be attributed to both, the finite size of the fiber tip, as well as a spatial shift of the fiber tip during mode profile measurement. Transmission losses at a wavelength of 1550 nm for waveguides with two different widths are listed in Table 3. Given the small aspect ratio of the waveguides, polarization dependent losses are expected and are confirmed by measurement to be about 2–3 dB/cm.

As seen in Table 3, when the width of the waveguide increases, the optical propagation loss increases. This can be attributed to the increased coupling into lossy higher order modes in wider waveguides. In addition, channel waveguides patterned by lift-off show lower loss compared to the channel waveguides defined by plasma etching techniques and this is attributed to better wave-

Table 2
Ratios of the different bands in the micro Raman fitted spectra

| Band located at ($cm^{-1}$) | As-deposited $Ge_{23}Sb_7S_{70}$ film | $Ge_{23}Sb_7S_{70}$ waveguide defined by $CHF_3$ plasma etching | $Ge_{23}Sb_7S_{70}$ waveguide defined by $SF_6$ plasma etching | $Ge_{23}Sb_7S_{70}$ waveguide fabricated by lift-off |
|---|---|---|---|---|
| 295 ($SbS_3$) | 23 | 20 | 21 | 23 |
| 304 (Substrate) | 1 | 2 | 1 | 1 |
| 323 (Corner-sharing $GeS_{4/2}$) | 22 | 22 | 23 | 22 |
| 340 ($GeS_4$) | 24 | 27 | 26 | 24 |
| 375 (Edge-sharing $GeS_{4/2}$) | 18 | 17 | 18 | 18 |
| 409 (Corner-sharing $GeS_{4/2}$) | 5 | 4 | 5 | 5 |
| 420 ($S_3Ge$–S–$GeS_3$) | 7 | 7 | 7 | 6 |

The fitting accuracy, limited by Raman measurement non-uniformity as well as the fitting method, is ±1% for all films measured.

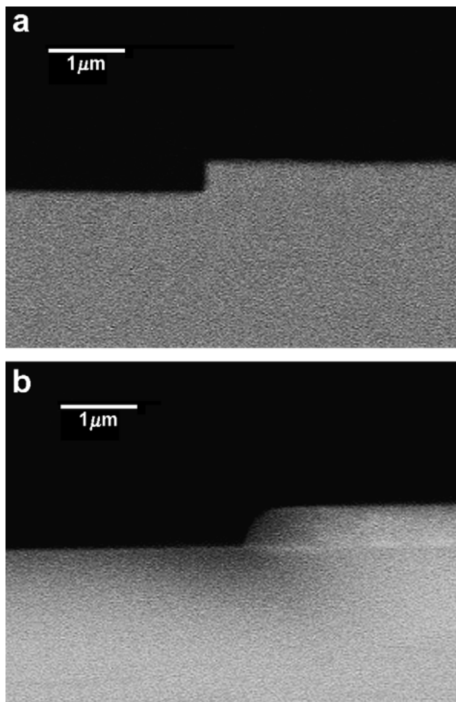


Fig. 3. Cross-sectional image of $Ge_{23}Sb_7S_{70}$ channel waveguide sidewall profile patterned by (a) $SF_6$ plasma etching, indicating vertical sidewall; and (b) lift-off, showing a sidewall angle of ~70° and rounded corners.

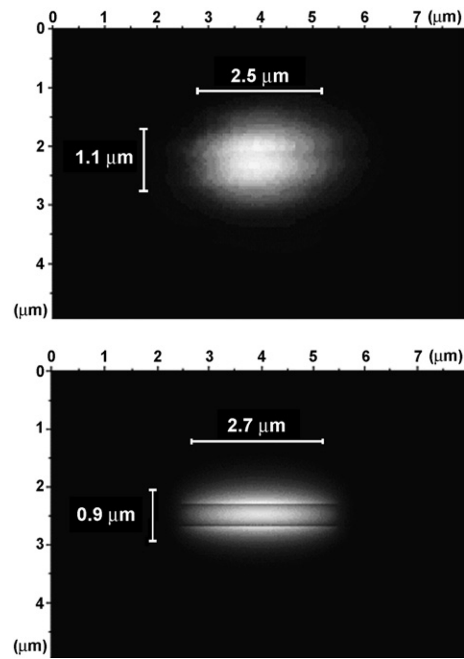


Fig. 4. (a) Measured TM-like mode profile of a 3 μm wide $Ge_{23}Sb_7S_{70}$ channel waveguide defined by $SF_6$ plasma etching, showing single mode operation; (b) Numerically simulated optical mode in 3 μm wide waveguide using finite-domain technique, showing good agreement with the measured results.

guide quality. Material absorption accounts for < 0.5 dB/cm optical loss as is confirmed by the loss measured in $Ge_{23}Sb_7S_{70}$ shallow rib waveguides [25], the residual loss excluding materials absorption is ~4 dB/cm in waveguides defined by $SF_6$ plasma etching and ~ 3 dB/cm for lift-off patterned waveguides. The lower loss in waveguide defined by lift-off has to be related to the better waveguide quality (e.g. smaller sidewall roughness, less defects from fabrication) resulting from lift-off technique. This conclusion is also consistent with our sidewall roughness measurement results.

## 5. Conclusion

In conclusion, we have demonstrated the successful fabrication of planar waveguides from thermally evaporated $Ge_{23}Sb_7S_{70}$ films using plasma etching and lift-off techniques. Fluorine based gas ($CHF_3$ and $SF_6$) plasma chem-

Table 3
Transmission loss (±0.4 dB/cm) and sidewall roughness (±2 nm) of $Ge_{23}Sb_7S_{70}$ channel waveguides patterned by different techniques (measured at 1550 nm by cutback technique): $CHF_3$ plasma etching, $SF_6$ plasma etching and lift-off

| | $CHF_3$ plasma etching | $SF_6$ plasma etching | Lift-off |
|---|---|---|---|
| Transmission loss of 3 μm wide channel waveguides (±0.4 dB/cm) | 4.1 dB/cm | 4.1 dB/cm | 3.0 dB/cm |
| Transmission loss of 4 μm wide channel waveguides (±0.4 dB/cm) | 4.8 dB/cm | 4.5 dB/cm | 3.6 dB/cm |
| Waveguide RMS sidewall roughness | 20 ± 5 nm | 17 ± 4 nm | 10 ± 2 nm |

istries have been found to be effective in defining fine waveguide structures in $Ge_{23}Sb_7S_{70}$ with high etching rates and vertical sidewall profiles. Micro-Raman spectroscopy has been utilized to compare the structure of the waveguides fabricated using different techniques. We have demonstrated that, during the fabrication of the waveguide, the lift-off technique does not change the structure of the film whereas slight structure modifications have been observed by Raman spectroscopy in waveguides after plasma etching. Using AFM, we have measured sidewall RMS roughness values of $20 \pm 5$ nm, $17 \pm 4$ nm and $10 \pm 2$ nm for $Ge_{23}Sb_7S_{70}$ waveguides defined by $CHF_3$ plasma etching, $SF_6$ plasma etching and lift-off, respectively. Accordingly, we have shown that waveguides defined by lift-off exhibit lower propagation loss than those patterned by plasma etching, which has been related to the better waveguide quality resulting from the lift-off recipe we employed.

This study has allowed us to demonstrate that standard waveguide fabrication techniques, especially lift-off, are a good choice for chalcogenide glass patterning in microphotonics, optical memory and sensor applications.

Disclaimer

This paper was prepared as an account of work supported by an agency of the United States Government. Neither the United States Government nor any agency thereof, nor any of their employees, makes any warranty, express or implied, or assumes any legal liability or responsibility for the accuracy, completeness or usefulness of any information, apparatus, product or process disclosed, or represents that its use would not infringe privately owned rights. Reference herein to any specific commercial product, process, or service by trade name, trademark, manufacturer, or otherwise does not necessarily constitute or imply its endorsement, recommendation, or favoring by the United States Government or any agency thereof. The views and opinions of authors expressed herein do not necessarily state or reflect those of the United States Government or any agency thereof.

## Acknowledgements

Funding support is provided by the Department Of Energy under Award Number DE-SC52-06NA27341. The authors would like to thank Dr. Ning-ning Feng and Rong Sun at MIT for technical assistance and helpful discussions. The authors acknowledge Microsystems Technology Laboratories at MIT for fabrication facilities and the Center for Materials Science and Engineering at MIT for characterization facilities. This work made use of MRSEC shared facilities supported by the National Science Foundation under Award Number DMR-0213282 and NSF laser facility Grant #CHE-0111370.

## References

[1] J. Sanghera, L. Shaw, L. Busse, V. Nguyen, P. Pureza, B. Cole, B. Harbison, I. Aggarwal, R. Mossadegh, F. Kung, D. Talley, D. Roselle, R. Miklos, Fiber Integr. Opt. 19 (2000) 251.
[2] L. Busse, J. Moon, J. Sanghera, I. Aggarwal, Laser Focus World 32 (1996) 143.
[3] A. Ganjoo, H. Jain, J. Ryan, R. Song, R. Chanda, J. Irudyraj, Y. Ding, C. Pantano, Proc. SPIE 5593 (2004) 637.
[4] O. Efimov, L. Glebov, K. Richardson, E. Van Stryland, T. Cardinal, S. Park, M. Couzi, J. Bruneel, Opt. Mater. 17 (2001) 379.
[5] J. Viens, C. Meneghini, A. Villeneuve, T. Galstian, E. Knystautas, M. Duguay, K. Richardson, T. Cardinal, J. Lightwave Technol. 17 (1999) 1184.
[6] Y. Ruan, W. Li, R. Jarvis, N. Madsen, A. Rode, B. Luther-Davies, Opt. Express 12 (2004) 5140.
[7] J. Frantz, L. Shaw, J. Sanghera, I. Aggarwal, Opt. Express 14 (2004) 1797.
[8] A. Mairaj, C. Riziotis, A. Chardon, P. Smith, D. Shepherd, D. Hewak, Appl. Phys. Lett. 81 (2002) 3708.
[9] N. Ponnampalam, R. DeCorby, H. Nguyen, P. Dwivedi, C. Haugen, J. McMullin, S. Kasap, Opt. Express 12 (2004) 6270.
[10] L. Zou, B. Chen, L. Chen, Y. Yuan, M. Hamanaka, M. Iso, Appl. Phys. Lett. 88 (2006) 153510.
[11] J. Hu, V. Tarasov, N. Carlie, L. Petit, A. Agarwal, K. Richardson, L. Kimerling, Opt. Express 15 (2007) 2307.
[12] W. Li, Y. Ruan, B. Luther-Davies, A. Rode, R. Boswell, J. Vac. Sci. Technol. A 23 (2005) 1626.
[13] R. Vahalova, L. Tichy, M. Vlcek, H. Ticha, Phys. Status Solidi A 181 (2000) 199.
[14] L. Petit, N. Carlie, F. Adamietz, M. Couzi, V. Rodriguez, K.C. Richardson, Mater. Chem. Phys. 97 (2006) 64.
[15] T. Asami, K. Matsuishi, S. Onari, T. Arai, J. Non-Cryst. Solids 211 (1997) 89.
[16] N. Carlie, J. Hu, L. Petit, A. Agarwal, L. Kimerling, A. Rode, B. Luther-Davies, K. Richardson, in preparation.
[17] O. Joubert, P. Paniez, M. Pons, J. Pelletier, J. Appl. Phys. 70 (1991) 977.
[18] C. Huang, D. Hewak, J. Badding, Opt. Express 12 (2004) 250.
[19] Q. Mei, J. Saienga, J. Schrooten, B. Meyer, S. Martin, J. Non-Cryst. Solids 324 (2003) 264.
[20] C. Julien, S. Barnier, M. Massot, N. Chbani, X. Cai, A. Loireau-Lozac'h, M. Guittard, Mat. Sci. Eng. B 22 (1994) 191.
[21] B. Frumarova, P. Nemec, M. Frumar, J. Oswald, M. Vleck, J. Non-Cryst. Solids 256–257 (1999) 266.
[22] P. Boolchand, J. Grothaus, M. Tenhover, M. Hazle, R. Grasselli, Phys. Rev. B 33 (1996) 5421.
[23] S. Campbell, The Science and Engineering of Microelectronic Fabrication, Oxford University Press, 1996.
[24] C. Xu, W. Huang, M. Stern, S. Chaudhuri, IEE Proc. Optoelectron. 141 (1994) 281.
[25] J. Hu, V. Tarasov, N. Carlie, L. Petit, N. Feng, A. Agarwal, K. Richardson, L. Kimerling, Si-CMOS-compatible lift-off fabrication of low-loss planar chalcogenide waveguides, Opt. Express 15 (2007) 11798.